Monthly Notices of the ROYAL ASTRONOMICAL SOCIETY

MNRAS **530,** 3570–3577 (2024) https://doi.org/10.1093/mnras/stae1062
Advance Access publication 2024 April 19

Observation of the L5 Kordylewski dust cloud with a portable imaging polarimetric telescope in the Namibian Khomas Highland

Judit Slíz-Balogh [1,2,3] Attila Mádai [1] Pál Sári [1,4] András Barta [3] and Gábor Horváth [1,3]★

[1] *Astropolarimetry Research Group, Office of Supported Research Groups, HUN-REN-ELTE, Hungarian Research Network, H-1052 Budapest, Piarista utca 4, Hungary*
[2] *Department of Astronomy, ELTE Eötvös Loránd University, H-1117 Budapest, Pázmány sétány 1, Hungary*
[3] *Environmental Optics Laboratory, Department of Biological Physics, ELTE Eötvös Loránd, University, H-1117 Budapest, Pázmány sétány 1, Hungary*
[4] *Fornax 2002 Ltd., H-2119 Pécel, Ady Endre utca 1, Hungary*

Accepted 2024 April 16. Received 2024 April 3; in original form 2023 December 9

ABSTRACT

The Kordylewski dust clouds (KDCs) around the L5 and L4 Lagrange points of the Earth–Moon system have been first observed by imaging polarimetry in 2017 and 2022 in a Hungarian astronomical observatory. Due to the non-ideal (almost always hazy, aerosol-polluted) astroclimate of Hungary and the extremely low intensity of dust-scattered sunlight, the polarimetric hunt after both KDCs lasted 2–7 yr. Waiting for cloud- and aerosol-free atmosphere and appropriate astronomical conditions (e.g. moonless sky with above-horizon KDC) in our Hungarian observatory takes a long time. Thus, our goal was to build a portable imaging polarimetric, wide field-of-view telescope and use it in the very good astroclimate of the Isabis Astro Lodge in the Khomas Highland of Namibia. Our long term aim is to study the dynamics of KDCs with this instrument in Namibian 1-month astropolarimetric campaigns in the next decade. In this work, we describe our portable imaging polarimetric telescope and present our first KDC observation achieved with it in Namibia during our 4-week astropolarimetric campaign between 2023 July 18 and August 15. We conclude that our portable polarimetric telescope functions well. Using it in Namibia, we corroborated the existence of the L5 KDC, the polarization characteristics (polarization degree and angle) of which refer to an inhomogeneous dust cloud composed of several particle agglomerations that scatter and linearly polarize the illuminating sunlight.

Key words: polarization – instrumentation: polarimeters – methods: observational – celestial mechanics – Earth – Moon.

1 INTRODUCTION

Although theoretically the two triangular Lagrange points L4 and L5 (Szebehely 1967) in the gravitational field of the Earth and Moon are stable, the gravitational perturbation of the Sun may disrupt this stability. The Sun–Earth–Moon–Particle restricted four-body model has recently been computationally modelled by Slíz et al. (2015, 2017), Salnikova, Stepanov & Shuvalova (2016, 2018), Slíz-Balogh, Barta & Horváth (2018), and Slíz-Balogh et al. (2022, 2023a). These models showed that on astronomical time-scale even if the Sun sweeps out many particles from the neighbourhood of these Lagrange points, during a less time (e.g. 30–40 yr) a considerable number of particles remain near the L4 and L5 points.

The two particle clouds around the L4 and L5 points of the Earth–Moon system were discovered in 1961 by the Polish astronomer, Kazimierz Kordylewski (Kordylewski 1961), after whom they were named as Kordylewski dust clouds (KDCs). In the 1960s and 70s there were many visual and/or photometric observations of the KDCs by Simpson (1967), Vanysek (1969), Roach (1975), and Winiarski (1989), but no photographs have been published. Due to the lack of convincing photometric evidence of the KDCs, some astronomers became sceptical about the existence of both dust clouds.

Using ground-based imaging polarimetry, Slíz-Balogh, Barta & Horváth (2019) and Slíz-Balogh et al. (2023a) presented the first (polarimetric) evidence of the existence of the L5 and L4 KDCs of the Earth–Moon system. Recently, Wang et al. (2021) summarized the results of the ground- and space-born KDC observations.

From 1961 to now the L4 and L5 KDCs were observed altogether 24 times: 19 times by naked eyes or photometrically and 5 times polarimetrically, within these the L5 KDC has been sighted 18 times, while the L4 KDC only 6 times. The two main reasons for this very few KDC observations are the extremely faint dust-scattered sunlight and the large extent (at least $15^\circ \times 15^\circ$) of both dust clouds. Therefore, such observations demand not only a cloudless sky, lack of astronomical light pollution, and aerosol-free air, but also a much larger telescope's field of view than that of usual polarimetric telescopes with a typical field of view of $1^\circ \times 1^\circ$ (Mignani et al. 2019).

The first ground-based polarimetric observations of the L5 and L4 KDCs were performed in 2017 and 2022 in Hungary, under the hazy, aerosol-polluted atmosphere of the Carpathian Basin having an unfavourable astroclimate. Although these observations were successful, waiting for ideal atmospheric (i.e. cloudless and aerosol-free) and astronomical (e.g. moonless and one of the KDCs is above

★ E-mail: gh@arago.elte.hu

the horizon) conditions took a long time (years), which could not ensure the study of the dynamics of the KDCs. To overcome this disadvantage, we looked for a place with a good astroclimate for ideal KDC observations. We found the Isabis Astro Lodge in the Khomas Highland of Namibia with a desert climate. Due to its ideal astroclimate, this site is also the home of the following astronomical projects: (i) High Energy Stereoscopic System (H.E.S.S.) conducted by the Max Planck Institute for Nuclear Physics (Heidelberg) detecting Cherenkov radiation from the atmosphere (Aharonian et al. 2023), (ii) Hungarian Automated Telescope Network in the Southern hemisphere (HATnet-South) searching for exoplanets (Hartman et al. 2020), and (iii) Russian Space Debris Monitoring Station.

The scientific motivation of our research is two-fold: Our first goal was to build a portable imaging polarimetric, wide field-of-view telescope (Fig. 1), and to use it in the very good astroclimate of the Namibian Khomas Highland. Our second, long-term aim is to investigate the dynamics of KDCs with this new telescope in 1-month Namibian astropolarimetric campaigns in the next decade. In this work, we first describe our portable imaging polarimetric telescope, and then present our first KDC observation achieved with it in Namibia during our 4-week astropolarimetric campaign between 18 July and 15 August (Namibian winter) 2023.

2 METHOD

2.1 Location

In the Isabis Astro Lodge (16°28′55" East, 23°26′19" South, altitude ~1800 m, Khomas Highland, Namibia), polarization pictures were taken (exposure: 360 s) about the L5 triangular Lagrange point of the Earth–Moon system and its surrounding of 15.26° (horizontal) × 10.18° (vertical) when the sky was cloudless and aerosol-free. The reasons for this Namibian choice are the followings: The three main requirements for a good astroclimate are: (i) good atmospheric transparency (in other words, low extinction and low dispersion due to small amounts of suspended dust and mist in the air; this can be achieved from higher altitudes above sea level), (ii) very low level of light pollution (rare population in the surroundings), and (iii) good seeing (low level of atmospheric turbulence). Since the Kordylewski dust clouds are extremely low-brightness celestial objects, the first two prerequisites are the most important. Therefore, dry (semi)desert locations are an ideal possibility. Further important considerations are: (i) altitude of the target object above the horizon, (ii) altitude above sea level, (iii) easy accessibility of the location, (iv) necessary infrastructure (power supply, internet, etc.), (v) minimal light pollution, and (vi) high number of clear nights.

For presenting the relative difference between our local (Hungarian) and Namibian opportunities regarding the quality of the sky background, we used the so-called 'Sky Quality Meter' (SQM) device for the quantitative measurement of this parameter. In Hungary, we made our KDC measurements under night skies with ~20.00 mag arcsec^{-2} (level 5 in Bortle scale, rarely ~20.80), but in Namibia we had chances to take the advantages of the nocturnal sky with ~21.85–21.95 mag arcsec^{-2} (level 1 in Bortle scale).

For these requirements and considerations our ideal choice was the Isabis Astro Lodge in Namibia, partly because it is far from any city lights (the nearest town is over 70 km away) and there are more than 300 clear nights per year. Quite understandably, in the immediate vicinity there are two astronomical stations: The older one is the H.E.S.S. observatory (16°30′00″ East, 23°16′17″ South; e.g. Aharonian et al. 2023) of the Max Planck Institute of Nuclear Physics (Heidelberg, Germany). The second one is the HATnet-South station (16°30′00″ East, 23°16′17″ South; e.g. Hartman et al. 2020).

2.2 Instruments

The motor-driven German Equatorial Fornax 51 Telescope Mount (Fornax Ltd., Pécel, Hungary) was controlled with an accurate tracking correction system called Telescope Drive Master (MDA-Invent Kft., Érd, Hungary). The Fornax mechanics was manually and automatically guided by an FS-2 controller and a SKYTOOLS 4 software, respectively. We used a full-frame (24 mm × 36 mm), extremely sensitive, back-illuminated astrocamera possessing a cooled monochromatic CMOS sensor (Moravian C3-61000EC Pro, Moravian Instrument, Zlin, Czech Republic) equipped with a built-in filter wheel having five filter positions after the objective lens. In this wheel, three linearly polarizing filters (Bresser GmbH., Rhede, Germany) with 0°, 60°, and 120° angles of their transmission axes from an arbitrary reference direction were set. We chose a Sigma 135 mm/F1.8 Art telephoto lens. For precise setting of the telescope's rectascension axis pointing to the South Pole a special camera, named Pole Master (QHYCCD, Beijing, China), was used. A self-produced Bathinov mask was used to set precisely the camera focus. We calibrated the astrophotographs with the usual bias, dark, and flat images.

We used the Moravian C3-61000 Pro EC (enhanced cooling) camera (cooled back-illuminated Sony IMX455 CMOS mono FF sensor, quantum efficiency > 87 per cent, dark current = 0.014 e-pixel^{-1} s^{-1}@0° C, $\Delta T_{\max} = -45°$ C) in 1 × 1 bin mode with a gain factor of 2750 to achieve the smallest self-noise, with a read-noise of 1.46 e- (root mean square), even if this narrows the dynamic range of the image somewhat. This extremely low noise also ensures that extremely faint (and non-point-like) objects are displayed in the pictures (signal-to-noise ratio >3).

We have made and processed the images by the MAXIM DL software. During their post-processing, we calibrated the light images with bias, dark, and flat frames (inclusive flat-darks). We took $N \times 10$ pieces of dark frames, separated according to several 'standard' temperatures and durations, from which we made N pieces of master-darks (median average). Since the dark and bias calibration images were separated with the help of the mentioned software, so-called thermal image calibration could also be performed, which ensures correct calibration even for exposure times different from the set standard durations. But, in spite of this feature and in order to increase the accuracy, we also took the light images using exactly the standard exposure times, in order to eliminate the possible inaccuracy of the dark current interpolation algorithm. The above-mentioned method provided the most accurate dark calibration available.

The polarization images taken through the three different-axis polarizers were evaluated with the ALGONET software developed by the Estrato Research and Development Ltd. (the director of which is one of the authors, AB). ALGONET is a general-purpose visual algorithm development and evaluation software, which is composed of a framework for managing the user interface and a large number of modules that can be combined to arbitrarily for any visual algorithmic purposes. We used ALGONET for the calibration of our polarimeter in the laboratory and for the evaluation of the polarization images taken in the field. This sotware can use 'fits' files as inputs, and can perform polarimetric operations using Stokes vectors and Mueller matrices. The same software was used in our earlier astropolarimetric measurements (Slíz-Balogh et al. 2019, 2023a).

Figure 1. Photograph of the measurement site of our observations performed with the portable polarimetric telescope at the Isabis Astro Lodge in the Namibian Khomas Highland.

According to the test of our polarimetric telescope and the evaluation of its polarization images, the net uncertainties Δp and $\Delta\alpha$ of the measured degree of linear polarization p and angle of polarization α of light transmitted through a linearly polarizing sheet (P-ZN/R-12628, Schneider, Bad-Kreuznach, Germany) with different transmission directions γ (= 0°, 45°, 90°, 135° from an arbitrary reference direction) in front of the objective lens are $\Delta p \approx \pm 1$ per cent, $\Delta\alpha \approx \pm 1°$. Possible error sources could be the photon-detection noise, induced polarization/cross-talk from the lens and differential pixel gains, for instance. We did not quantify (i) the noise level in fractional polarization (*Q*/*I*, *U*/*I*), (ii) the contribution due to detector noise, and (iii) how these noises propagate to the final net p- and α-values. We did not determine the individual contributions of these error sources to the net absolute errors Δp and $\Delta\alpha$, because we are interested only in the net p and α patterns of the KDC. Note also that all optically relevant characteristics of the used detector (quantum efficiency > 87 per cent, 0.014 e- pixel^{-1} s^{-1} @0° C dark current, 1.46 e- read-noise RMS @ 2750 gain factor) were excellent, ensuring extremely low self-noise and signal-to-noise ratio larger than 3. After evaluation of the three polarization pictures of the linearly polarizing sheet taken through the three linearly polarizing filters (with 0°, 60°, and 120°) we expected homogeneous patterns with $p = 100$ per cent and $\alpha = \gamma$. And indeed, both measured p- and α-patterns of the polarizing sheet with a given γ were homogeneous with 98 per cent $\leq p \leq 100$ per cent, and for example $44° \leq \alpha \leq 46°$ for $\gamma = 45°$. From these $p = 99$ per cent ± 1 per cent and $\alpha = 45° \pm 1°$ follow, on the basis of which we concluded $\Delta p \approx \pm 1$ per cent and $\Delta\alpha \approx \pm 1°$ uncertainties.

To exclude the possibility of instrumental polarization effects, with our polarimetric telescope we also measured the patterns of the degree p and angle α of polarization of sky around the zenith immediately after sunset. Under this illumination conditions the scattered skylight dominates and the contribution of any light source from outside the Earth's atmosphere is irrelevant. Using our polarimetric telescope, we obtained the same well-known celestial polarization patterns around the zenith as measured earlier with other imaging polarimeters and reviewed by Horváth, Barta & Hegedüs (2014). This also demonstrated convincingly that there is no instrumental polarization artefact in our polarimetric telescope. In sum, the mentioned uncertainties (±1 per cent, ±1°) are not (i) time-variable residuals after calibration, (ii) variations of the instrumentally induced polarization across the field of view, and (iii) measured polarization signals for unpolarized stars.

3 RESULTS

Fig. 2 shows the polarization patterns of the L5 KDC measured with imaging polarimetry. In Fig. 2(b–d), the inner rectangle represents the sky window of the earlier polarimetric observations of the L5 KDC performed by Slíz-Balogh et al. (2019, 2023a). This KDC was detected on 2023 August 12 at 02:24:04 UT with dust cloud phase 61 per cent (= portion of the sunlit part of the disc of the real Moon, if it were in the same position as the KDC) and phase angle $\beta = 75.5°$. In Fig. 2(b), no structure is discernible in the very faint scattered light. However, in the pattern of the degree of linear polarization p, in four elongated zones seven diffuse conglomerata of black pixels with 5 per cent $\leq p \leq$ 20 per cent are seen around the L5 Lagrange point. The same conglomerata of red pixels with $81° \leq |\alpha| \leq 90°$ are also visible in the patterns of the angle of polarization α. This striped pattern recalls the similar striped structure of computer-modelled L5 KDC (Slíz-Balogh et al. 2018). Compared to the first three observations of the L5 KDC, this striped structural similarity is more striking in our fourth observation due to the 2 × 2-times larger field of view of our new polarimetric telescope used in Namibia. The multiple-striped structure is presumably the result of a gravitational mean motion resonance with Moon, which resonance is similar to that occurring in the Sun–Jupiter-particle system for particles uniformly launched from the vicinity of the L4 and L5 Lagrange points of the Sun–Jupiter system (Slíz-Balogh, Horváth & Horváth 2023b).

Fig. 2(e) displays the α-pattern of Fig. 2(d) with white bars representing the local directions of polarization together with the scattering plane (yellow line) and the plane perpendicular (white line) to the latter. These bars are practically orthogonal to the plane of scattering. This orthogonal direction proves that the light of the L5 KDC is the result of the scattering of sunlight on the dust particles. Figs 2(c–e) present the fourth polarimetric measurement of the L5 KDC of the Earth–Moon system after the first, second (2017 August 17 and 18; Slíz-Balogh et al. 2019), and third (2021 October 31; Slíz-Balogh et al. 2023a) observations.

Figs 2(f and g) show the normalized frequencies of p and α of the L5 KDC, respectively, measured on 2023 August 12 at 02:24:04 UT. The most frequent and the maximal p-value is 6 per cent and about 20 per cent, respectively, and the peak of the α-curve is at 90° from the scattering plane (Fig. 2f) referring to the scattering of sunlight on the KDC's particles.

Fig. 3 shows the geometry, photograph, the p- and α-patterns, and the distributions of p and α measured at 00:53:32 UT on 2023 August 13 when the L5 point was not within the same celestial window as that of Figs 2(b–e). The most frequent p-value is 2 per cent (Fig. 3f), which is practically negligible. The peak of the α distribution is at an angular distance of 80° from the direction of the scattering plane (Fig. 3g). The half band width of the p distribution is 5 per cent, while in Fig. 2(f) it is 12 per cent. On the other hand, the half band width of both α distributions in Figs 2(g) and 3(g) is 10°. The photograph (Fig. 3b) as well as the p- (Fig. 3c) and α-patterns (Figs 3d, e) are structureless: apart from the bright celestial bodies, the radiance is homogeneous dark, the most frequent p is very low (p = 2 per cent) and the direction of polarization is not perpendicular to the scattering plane. Hence, in Fig. 3 the polarization patterns are practically homogeneous and unpolarized. This refers to the absence of the L5 KDC in this celestial window.

Fig. 4 compares the polarization patterns of the L5 KDC measured earlier by Slíz-Balogh et al. (2019) (Figs 4b, c, e, f) and Slíz-Balogh et al. (2023a; Figs 4h, i) with those (Figs 4k, l) in the inner rectangle of Figs 2(c, d) of our present measurement. Due to the similar phase angles β (= 73.0°, 87.3°, 73.1°, 77.5°), the polarization signal of the L5 KDC is strong in all four cases, because the nearer is β to 90°, the higher is the degree of polarization p of light scattered by the dust particles. Apart from the necessary ideal astroclimate, this is the main reason for these successful polarimetric detections of the L5 KDC. Most importantly, in all four observations the KDC has multiple stripes composed of several conglomerates/aggregations, as was predicted by computer modelling of KDC formation (Slíz-Balogh et al. 2018). In the patterns of the degree of linear polarization p (Figs 2c, 3c, 4b, e, h, k) the stars (usually emitting practically unpolarized light) occur as non-polarized ($p \approx 0$ per cent) points/spots coded by white according to the used grey colour scale.

On 2023 August 12, we detected the L5 KDC with $\beta = 77.5°$ (Fig. 2), when the most frequent p-value was $p_{\mathrm{peak,\,L5}} = 6$ per cent (Fig. 2f). Comparing the new $p_{\mathrm{peak}} = 6$ per cent at $\beta = 77.5°$ with the previous $p_{\mathrm{peak}} = 6, 7, 4, 4$ per cent at β = 73.0°, 87.3°, 77.5°, 73.1° in Figs 4(c, g, k, o) (Slíz-Balogh et al. 2019, 2023a), we can conclude that usually, the closer is β to 90°, the higher is p. This trivially follows from the well-known law that the degree of linear polarization p of first-order-scattered light increases with increasing scattering angle β (Können 1985, Coulson 1988).

On the basis of the above results, we conclude that our portable polarimetric telescope functions well. Using it in Namibia, we corroborated the existence of the L5 KDC, the polarization characteristics (polarization degree and angle) of which refer to an inhomogeneous dust cloud composed of several particle agglomerations that scatter and linearly polarize the illuminating sunlight.

4 DISCUSSION

In our first astropolarimetric campaign in the Namibian Isabis Astro Lodge, we had one successful polarization observation of the L5 KDC of the Earth–Moon system despite some initial technical problems. Although this site has one of the best astroclimates on Earth (during our measurements the sky brightness was 21.82 mag arcsec^{-2}, being level 1 in Bortle Scale), even there it was not possible to detect the KDCs with photometry. However, we provided a positive polarimetric detection of inhomogeneous structures around the L5 point of the Earth–Moon system on 2023 August 12.

The computer simulations of Salnikova et al. (2016, 2018) and Slíz-Balogh et al. (2018) showed, that the KDCs around both Lagrange points (L4, L5) have extended, time-changing structures resulting from the aggregation/trapping of interplanetary dust. The dust clouds illuminated by direct sunlight can evidently be detected from the Earth surface with sufficiently polarization-sensitive detectors (Slíz-Balogh et al. 2019, 2023a). After Kordylewski's (1961) first photometric observation of dust clouds, suddenly a great interest arose in them in the 1960s, 70s, and 80s. There were several sightings, mainly in Arizona (Vanysek 1969; Roach 1975; Winiarski 1989), but none of the photos were of publishable quality. The best photometric or naked-eyed visibility of the KDCs is at 'full dust moon', when the phase angle β (defined by the Sun, KDC, and observer) is small and the degree of polarization p of the dust-scattered sunlight is zero. On the contrary, the polarimetric observation is optimal at 'half dust moon', when $\beta \approx 90°$ and p is maximal. Therefore, for KDC polarimetry it was necessary to look for a situation where $\beta \approx 90°$.

Sunlight scattered by dust particles becomes partially linearly polarized perpendicular to the scattering plane passing through the Sun, the observer, and the dust (Können 1985; Coulson 1988; Collett 1994). Exactly this polarization feature occurred in the α-pattern of the L4 and L5 KDCs (Figs 2c, d, e). This is the most convincing

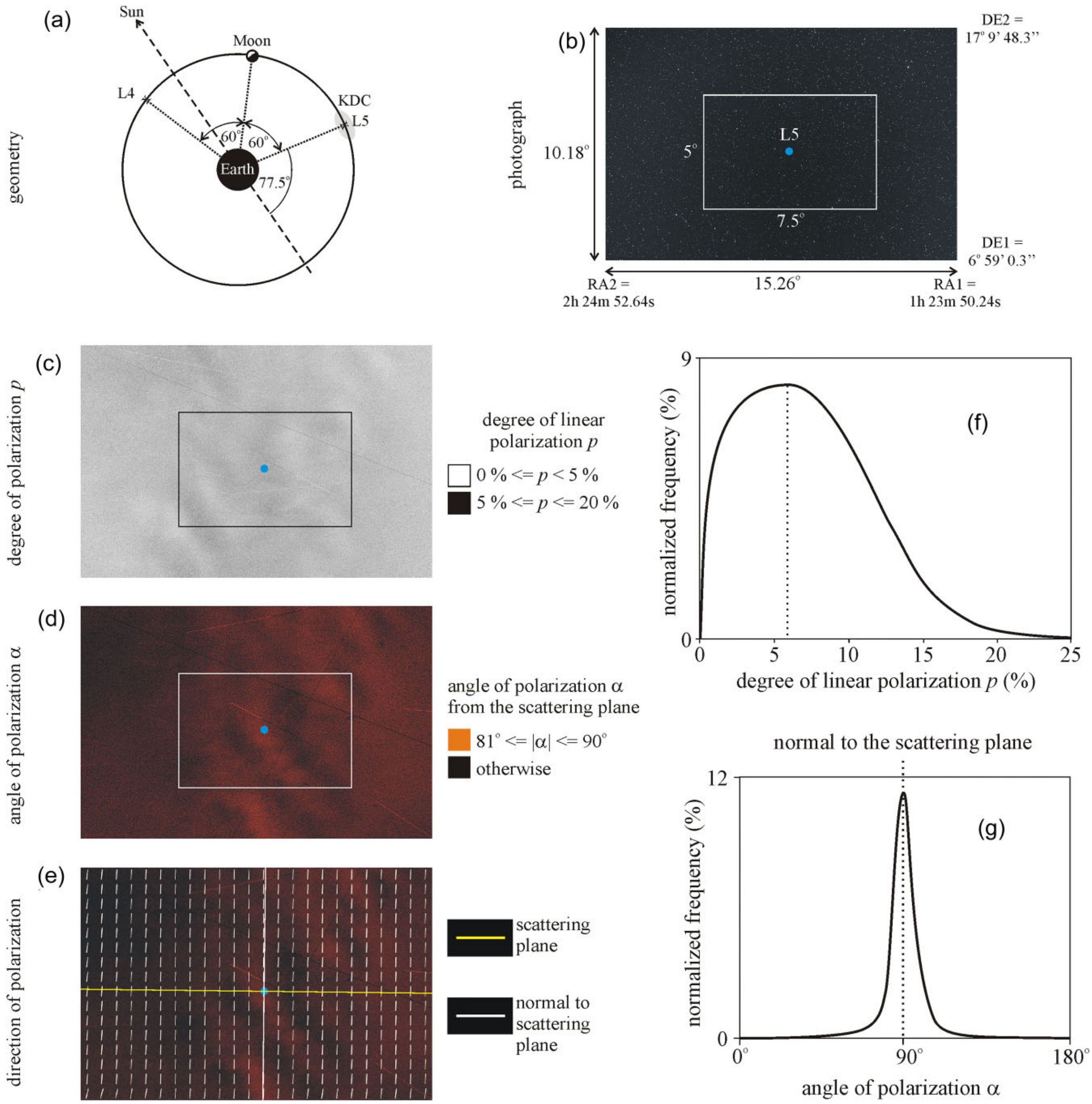

Figure 2. Imaging polarimetry of the Kordylewski dust cloud (KDC) at the L5 Lagrange point of the Earth–Moon system. (a): Geometry in the sky window studied on 2023 August 12 at 02:24:04 UT with dust cloud phase 61 per cent (= portion of the sunlit part of the disc of the real Moon, if it were in the same position) and phase angle $\beta = 75.5^{\circ}$. The angular relations and the extension of the KDC are real, while the dimensions of the Earth and Moon are not to scale. (b–e): Photograph, and patterns of the degree p and angle α (relative to the scattering plane shown by a yellow line in the α-patterns) of linear polarization of the sky around the L4 point measured by imaging polarimetry. Picture centre: RA = $01^{h}54^{m}21^{s}$, DE = $12^{\circ}04'24''$. The position of the L5 point is shown by a blue dot. (e): The white bars represent the local directions of polarization (averaged within the local rectangle, the side of which is the same as the bar's length), the yellow and white straights show the scattering plane and the perpendicular plane passing through the centre of the picture, respectively. Beyond the orthogonal white and yellow straights, the oblique lines in the p- and α-patterns are traces of satellites. (b–d): The inner rectangle represents the sky window of earlier polarimetric observations of the L5 KDC (Slíz-Balogh et al., 2019, 2023a). (f, g): Normalized frequencies (per cent = number of pixels with a given p- or α-value divided by the total number of pixels of the pattern) of p and α measured around the L5 point.

argument that we sensed dust-scattered sunlight originating from outside the Earth's atmosphere, rather than from the ground or the atmosphere. Another indication of KDC observation is that two to four dust conglomerates occur in the measured p- and α-patterns, as suggested by previous computer modelling (Slíz-Balogh et al. 2018).

Since our control polarization patterns (Fig. 3) measured when the L5 point was not in the studied sky window do not contain the typical, theoretically predicted KDC characteristics, we ruled out that the detected polarization signals did not originate from unwanted artificial lights reflected from telescope components or from the

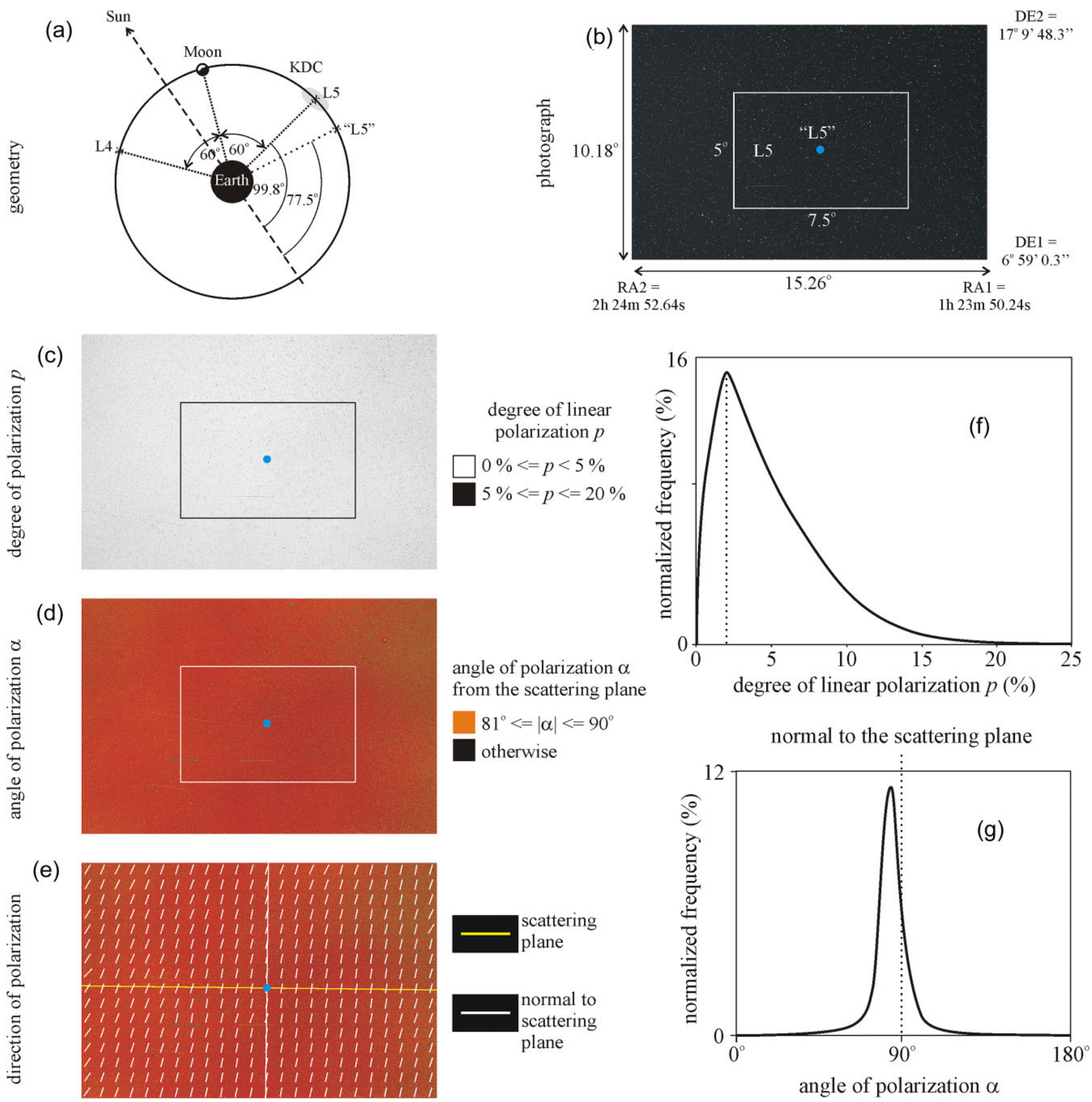

Figure 3. As Fig. 2 for the control measurement performed at 00:53:32 UT on 2023 August 13 (phase angle $\beta = 99.8°$, picture centre: RA = $01^{h}54^{m}21^{s}$, DE = $12°04'24''$) when the L5 point was not within this celestial window, therefore the blue dot 'L5' represents the earlier L5 position at 02:24:04 UT on 2023 August 12 (see Fig. 2b–e). (f, g): As Fig. 2f, g measured at 00:53:32 UT on 2023 August 13 when the L5 point was not within the same celestial window as that of Fig. 2b–e.

Earth. No specific structure could be recognized in these practically unpolarized, almost completely homogeneous control polarization patterns.

Earlier, Slíz-Balogh et al. (2019) also showed that the observed L5 KDC can be neither a cirrus cloud nor an aircraft contrail, because the polarization characteristics of these celestial phenomena are completely different from those of a KDC. Owing to these control measurements done during the first and second polarimetric observations of the L5 KDC on 2017 August 17 and 18, it was unnecessary to repeat these controls for the L5 KDC detected by us for the fourth time on 2023 August 12.

In Fig. 2(d) the polarization angle α varies slightly from point to point, resulting in the non-homogeneous α-pattern, the tiny inhomogeneities of which is visualized by the red–black colour distribution. Several main lobes of the L5 Kordylewski dust cloud come out by the spatially sudden and larger black–red differences. However, these fine α-variations are not apparent in Fig. 2(e), where the local angles of polarization are displayed by white bars aligned semiconstantly, almost vertically, perpendicular to the scattering plane. The reason for this apparent constant bar's direction is that the local α is averaged within the local rectangle, the side of which is

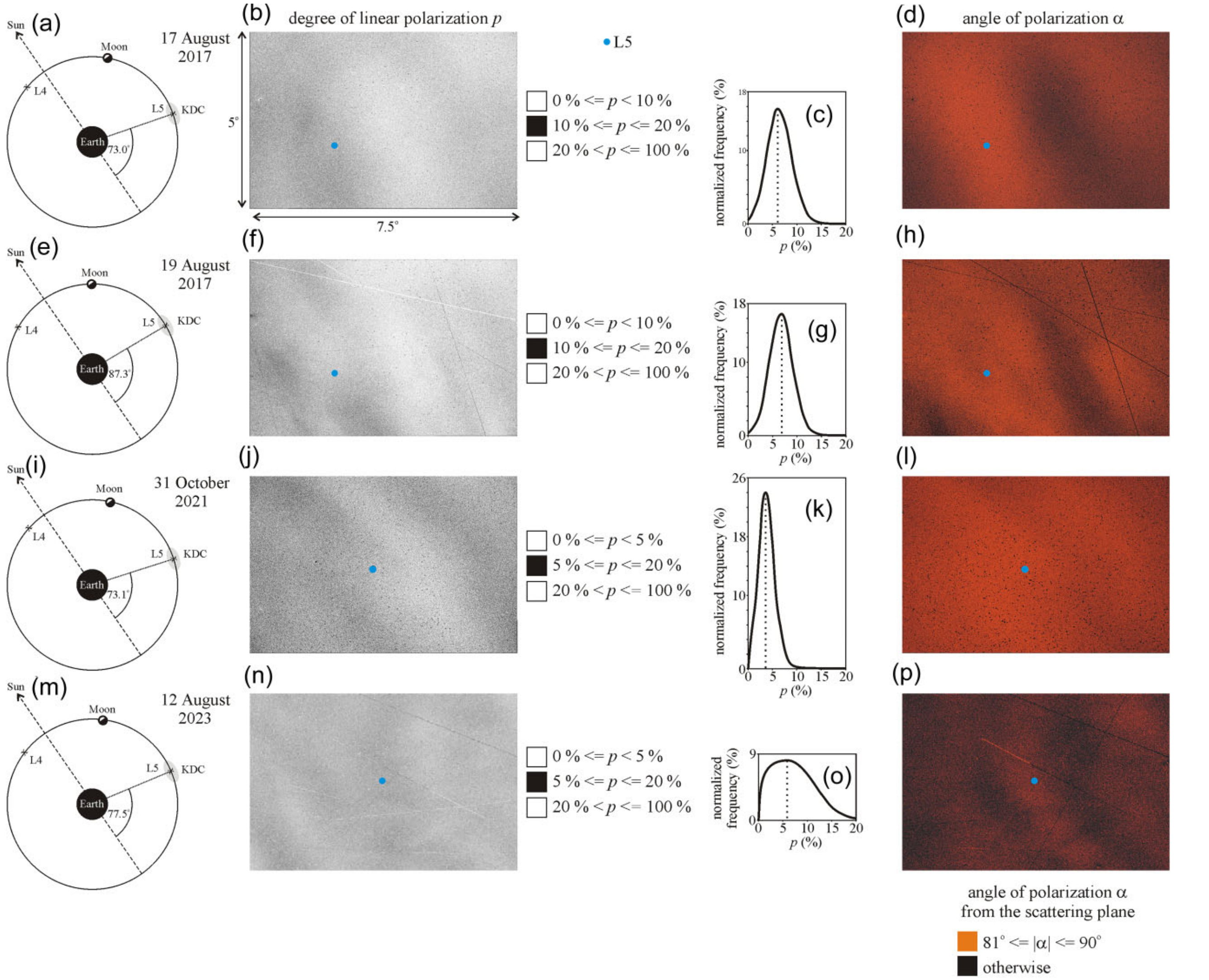

Figure 4. Comparison of the polarization patterns of the L5 KDC measured by Slíz-Balogh et al. (2019, 2023a) with those in the inner rectangle of Figs 2c, d. The L5 Lagrange point is depicted by a blue dot. Geometry (a, e, i, m), and patterns of the degree p (b, f, j, n) and angle α (d, h, l, p) of linear polarization. (c, g, k, o): Normalized frequencies (per cent = number of pixels with a given p-value divided by the total number of pixels of the pattern) of p measured around the L5 point. (a–d): 23:29:67 UT on 2017 August 17, phase angle $\beta = 73.0°$. (e–h): 01:14:15 UT on 2017 August 19, $\beta = 87.3°$. (i–l): 23:02:52 UT on 2021 October 31, $\beta = 73.1°$. (m–p): 02:24:04 UT on 2023 August 12, $\beta = 77.5°$.

the same as the length of the bar. Of course, this averaging more or less abolishes the fine, pixel-by-pixel variations of α.

Similarly to the earlier polarimetric KDC detections (Slíz-Balogh et al. 2019, 2023a), the consistent observation of the polarization angle α being perpendicular to the scattering plane from the Sun in Fig. 2(e) confirms the polarization detection of the L5 Kordylewski dust cloud. Note, that Fig. 3(e) shows a very similar α-pattern for a sky window that does not contain any Kordylewski cloud, and according to Fig. 3(c), in this sky window the degree of linear polarization $p \leq 2$ per cent is not zero. The cause of this very weakly polarized homogeneous signal cannot be sunlit gas, dust or clouds in the Earth's high atmosphere, because during our measurement at 00:53:32 UT, 2023 August 13 the Sun was by 82°12 arcmin below the horizon. Moreover, according to the preliminary polarization test of our portable polarimetric telescope, a possible instrumental polarization effect that favours vertical polarization is also out of question. The homogeneous and extremely weak p-pattern in Fig. 3(c) and α-patterns in Figs 3(d, e) – being only slight above the polarization sensitivity/accuracy of our polarimetric telescope – should originate from the inconspicuously polarized, faint sunlight scattered from the ambient interplanetary dust/particles. This faint light results in the well-known zodiacal light, for example (Gehrels 1974, Können 1985).

The Namibian site of our astropolarimetric observations was undoubtedly excellent due to its ideal astroclimate. A consideable portion of Namibia is still a desert prone to dusty conditions, that can cause more or less aerosol-rich skies. However, our measurement site, the Isabis Astro Lodge is in the Khomas Highland being horizontally far from the true dust deserts at an average height of about 1800 m above sea level and possessing mainly rocky and vegetation-covered surfaces. Consequently, the atmospheric aerosol/dust content is always very low above this site. This is one of the reasons why three other astronomical stations (German H.E.S.S., Hungarian HATnet-South, and Russian Space Debris Monitoring Station) function steadily in the vicinity (1–35 km) of the Isabis Astro Lodge. Thus, during our observations the atmospheric aerosol/dust content was surely negligible and had practically no influence on our polarimetric measurements.

Based on the experience of our previous KDC measurements, it seemed necessary to perform observations in a site with a more favourable astroclimate (with an aerosol-free atmosphere and cloudless sky) than that in Hungary, where the pre-requisite of an ideal astroclimate for such measurements occurs only on a few days per year. This is why we built a portable, imaging-polarimetric, wide field-of-view telescope and performed with it our first measurement campaign in 2023 July–August in the Namibian Isabis Astro Lodge (Khomas Highland) which we plan to repeat several times in the following years.

CONFLICT OF INTEREST

The authors declare no competing interest and have no conflict of interest.

ACKNOWLEDGEMENTS

We are very grateful to the family Joachim and Adele Cranz for the possibility that we could conduct our astropolarimetric campaign in their Isabis Astro Lodge on the Namibian Khomas Highland. We thank the valuable help of Ilona Mitró provided in Namibia. We thank an anonymous reviewer for her/his valuable and constructive comments on the earlier version of our paper.

This work was supported by the Office of Supported Research Groups of the Hungarian Research Network under the grant number HUN-REN-ELTE-0116607 Astropolarimetry.

DATA AVAILABILITY STATEMENT

The data underlying this article are available in the article which has no supplementary material.

REFERENCES

Aharonian F. et al., 2023, ApJ, 952, L38
Collett E., 1994, Polarized Light: Fundamentals and Applications, Marcel Dekker, New York
Coulson K. L., 1988, Polarization and Intensity of Light in the Atmosphere, A. Deepak Publishing, Hampton, VA
Gehrels T.ed., 1974, Planets, Stars and Nebulae Studied with Photopolarimetry, Univ. Arizona Press, Tucson, Arizona
Hartman J. D. et al., 2020, Astron. J., 159, 173
Horváth G., Barta A., Hegedüs R., 2014, in Horváth G., ed., Polarized Light and Polarization Vision in Animal Sciences, Springer, Berlin, p. 367
Kordylewski K., 1961, Acta Astron., 11, 165
Können G. P., 1985, Polarized Light in Nature, Cambridge Univ. Press, Cambridge
Mignani R., Shearer. A., Slowikowska A., Zane S, in 2019, Shore N. S., ed., Astrophysics and Space Science Library, Vol. 460, Astronomical Polarisation from the Infrared to Gamma Rays. Springer, Berlin
Roach J., 1975, Planet. Space Sci., 23, 173
Salnikova T. V., Stepanov S. Y., Shuvalova A. I., 2016, Dokl. Phys., 61, 243
Salnikova T., Stepanov S., Shuvalova A., 2018, Acta Astronaut., 150, 85
Simpson J. W., 1967, Phys. Today, 20, 39
Slíz J., Kovács T., Süli Á., 2017, Astronomical Notes, 338, 536
Slíz J., Süli Á., Kovács T., 2015, Astronomical Notes, 336, 23
Slíz-Balogh J., Barta A., Horváth G., 2018, MNRAS, 480, 5550
Slíz-Balogh J., Barta A., Horváth G., 2019, MNRAS, 482, 762
Slíz-Balogh J., Érdi B., Horváth D., Horváth G., 2022, Icarus, 374, 114814
Slíz-Balogh J., Horváth D., Horváth G., 2023b, Acta Astronaut., 211, 208
Slíz-Balogh J., Mádai A., Sári P., Barta A., Horváth G., 2023a, MNRAS, 518, 5236
Szebehely V., 1967, Theory of Orbits: The Restricted Problem of Three Bodies. Academic Press, New York
Vanysek V., 1969, Nature, 221, 47
Wang P. et al., 2021, Space Sci. & Technol., 2021, 6597921
Winiarski M., 1989, Earth, Moon and Planets, 47, 193

This paper has been typeset from a Microsoft Word file prepared by the author.